Auton Robot (2008) 25: 3–13
DOI 10.1007/s10514-007-9071-6

Controlling swimming and crawling in a fish robot using a central pattern generator

Alessandro Crespi · Daisy Lachat · Ariane Pasquier · Auke Jan Ijspeert

Received: 30 October 2006 / Accepted: 3 December 2007 / Published online: 22 December 2007

Abstract Online trajectory generation for robots with multiple degrees of freedom is still a difficult and unsolved problem, in particular for non-steady state locomotion, that is, when the robot has to move in a complex environment with continuous variations of the speed, direction, and type of locomotor behavior. In this article we address the problem of controlling the non-steady state swimming and crawling of a novel fish robot. For this, we have designed a control architecture based on a central pattern generator (CPG) implemented as a system of coupled nonlinear oscillators. The CPG, like its biological counterpart, can produce coordinated patterns of rhythmic activity while being modulated by simple control parameters.

To test our controller, we designed BoxyBot, a simple fish robot with three actuated fins capable of swimming in water and crawling on firm ground. Using the CPG model, the robot is capable of performing and switching between a variety of different locomotor behaviors such as swimming forwards, swimming backwards, turning, rolling, moving upwards/downwards, and crawling. These behaviors are triggered and modulated by sensory input provided by light, water, and touch sensors. Results are presented demonstrating the agility of the robot and interesting properties of a CPG-based control approach such as stability of the rhythmic patterns due to limit cycle behavior, and the production of smooth trajectories despite abrupt changes of control parameters.

The robot is currently used in a temporary 20-month long exhibition at the EPFL. We present the hardware setup that was designed for the exhibition, and the type of interactions with the control system that allow visitors to influence the behavior of the robot. The exhibition is useful to test the robustness of the robot for long term use, and to demonstrate the suitability of the CPG-based approach for interactive control with a human in the loop.

This article is an extended version of an article presented at BioRob2006 the first IEEE/RAS-EMBS International Conference on Biomedical Robotics and Biomechatronics.

Keywords Fish robot · Central pattern generator · Swimming · Crawling

A. Crespi (✉) · D. Lachat · A. Pasquier · A.J. Ijspeert
School of Computer and Communication Science, Ecole Polytechnique Fédérale de Lausanne (EPFL), Station 14, 1015 Lausanne, Switzerland
e-mail: alessandro.crespi@epfl.ch

D. Lachat
e-mail: daisy.lachat@epfl.ch

A. Pasquier
e-mail: ariane.pasquier@epfl.ch

A.J. Ijspeert
e-mail: auke.ijspeert@epfl.ch

1 Introduction

The agility and efficiency of animal locomotion tend to fascinate engineers. The skills to coordinate multiple degrees of freedom (DOFs), using compliant actuators (muscles and tendons), and massively parallel control (the central nervous system), give animals an agility and energy efficiency rarely replicated in man-made robots. One of the most impressive features of animals is their capability to rapidly modulate locomotion according to the environmental context. Indeed animals tend to continuously modify their locomotion, for instance to accelerate, decelerate, change direction, and/or change the type of gait. Another impressive feature is how they effortlessly deal with multiple redundancies: redundancies in the number of articulated joints, redundancies in the

musculature (there are multiple muscles acting on a single joint, and often single muscles acting on multiple joints) and redundancies in muscles (a single muscle is decomposed into multiple motor units).

To a large extent, the problem of dealing with these redundancies and with these modulations is solved by *central pattern generators*, i.e., neural networks capable of producing coordinated patterns of rhythmic activity without any rhythmic inputs from sensory feedback or from higher control centers (Delcomyn 1980). Even completely isolated CPGs in a Petri dish can produce patterns of activity, called fictive locomotion, that are very similar to intact locomotion when activated by simple electrical or chemical stimulation, (Grillner 1985). Typically, varying simple stimulation allows modulation of both the speed and direction of locomotion. From a control point of view, CPGs therefore implement some kind of feedforward controller, i.e., a controller that "knows" which torques need to be rhythmically applied to obtain a given speed of locomotion. Interestingly, CPGs combine notions of stereotypy (steady state locomotion tends to show little variability) and of flexibility (speed, direction and types of gait can continuously be adjusted).

In this article, we apply the concept of CPGs to the control of a novel fish robot. We are interested in testing how a CPG implemented as a system of coupled nonlinear oscillators can be used to control swimming and crawling. Our purpose is to demonstrate that such a system can be a useful basis for producing and modulating a variety of different locomotor behaviors, and for rapidly switching between them. Note that the CPG model presented in this article is not meant to model a particular biological system and only replicates biological principles at an abstract level. Note also that we do not claim that this dynamical systems approach outperforms alternative approaches, and our purpose is mainly exploratory (i.e., exploring the pros and cons of using CPGs in fish robots).

This work follows several related projects on the use of CPGs for controlling a quadruped robot (Billard and Ijspeert 2000), a lamprey/snake robot (Crespi and Ijspeert 2006; Ijspeert and Crespi 2007), a salamander robot (Ijspeert et al. 2007), and a humanoid robot (Righetti and Ijspeert 2006). A shorter version of this article has been published in the proceedings of BioRob2006, the first IEEE/RAS-EMBS International Conference on Biomedical Robotics and Biomechatronics (Lachat et al. 2006). The main additions compared to the shorter article are a more detailed presentation of the control architecture, new results on crawling and the description of the use of the robot in a public exhibition.

In the next sections, we first make a brief overview of related work (Sect. 2). We then present the design of our robot (Sect. 3), and its control architecture (Sect. 4). Experiments demonstrating different locomotor behaviors are presented in Sect. 5. In Sect. 6, we present the hardware and software extensions that have been carried out for the exhibition. Our approach is discussed in Sect. 7.

2 Related work

Multiple fish robots have been designed and realized. Most robots implement anguilliform or carangiform swimming modes, i.e., modes which use mainly the body and the tail for propulsion (Sfakiotakis 1999; Colgate and Lynch 2004). Ostraciiform or labriform modes, which use caudal and pectoral fins and almost no body motions, have been less studied. Relatively few fish robots are fully autonomous, capable of swimming in 3D and reacting to their environment. For instance, the well-known RoboTuna from MIT, which has been designed to study speed optimization, is attached to a horizontal guide (Triantafyllou and Triantafyllou 1995).

Several groups are very active in designing autonomous fish robots (Kato 2000; Liu et al. 2004; Yu et al. 2004). The National Marine Research Institute (NMRI) in Japan, for instance, is working on multiple projects, including maneuvering, swimming performance and modular robotics for water; each robot is built for a particular purpose like up-down motion, high turning performance, or high speed swimming.[1] The University of Essex developed a 3D swimming robotic fish called MT1, which is fully autonomous (Liu et al. 2005). A micro robotic fish actuated by PZT bimorph actuators has recently been built by the University of California, Berkeley (Deng and Avadhanula 2005), mimicking a boxfish.

Most of these robots are controlled using traditional control methods that combine (algorithmic) sine-based trajectory generators, and PID feedback controllers. Recently, the concept of CPG is increasingly used as an alternative approach for online rhythmic trajectory generation (Wilbur et al. 2002; Fukuoka et al. 2003; Nakanishi et al. 2004; Ijspeert et al. 2005). In most cases, the CPGs are implemented as recurrent neural networks or systems of coupled nonlinear oscillators.

CPGs have rarely been applied to the control of a swimming robot. To the best of our knowledge, previous examples have mainly addressed anguilliform swimming: Arena, Ayers, Dario's groups have independently used CPG models inspired by the lamprey locomotor network for producing travelling undulations in lamprey-like robots (Arena 2001; Wilbur et al. 2002; Stefanini et al. 2006); see also (Ijspeert and Crespi 2007). In this article, we would like to contribute to underwater robotics in several ways: (1) with the design of a novel fish robot capable of ostraciiform (and labriform) swimming modes and crawling, and (2) with a CPG-based controller that allows agile locomotion in a fully autonomous fish robot.

[1] Fish Robot Home Page of NMRI. URL: http://www.nmri.go.jp/eng/khirata/fish/index_e.html.

Fig. 1 BoxyBot (view from above)

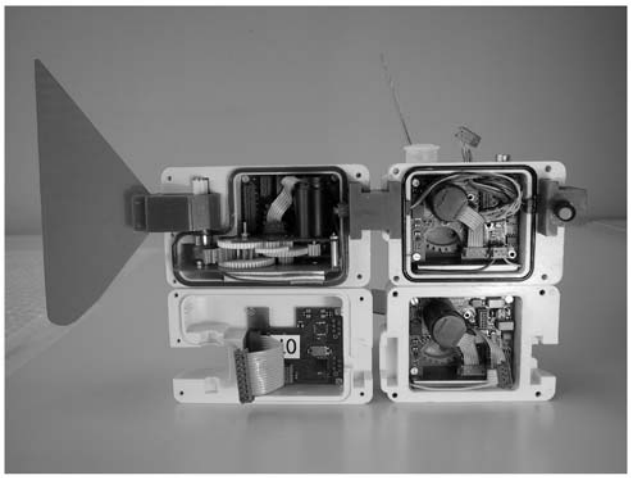

Fig. 2 View from side of the internal components of BoxyBot. The left side of the robot is placed above the right side. On the *left* is the body module with caudal fin and on the *right* is the head module with pectoral fins

3 The fish robot BoxyBot

3.1 Mechanical design

The body of the robot (Fig. 1) is loosely inspired from the boxfish (a fish living in coral reefs) and from the mudskipper (a fish capable of crawling on ground). The robot is made of two principal parts: the head module, providing two independent joints around the pitch axis (pectoral fins), and the body module, providing a joint around the yaw axis (caudal fin). The modules are rigid cases and are attached together with a rigid part (Fig. 2).

The fish robot is designed to implement labriform or ostraciiform swimming modes. Fishes that uses ostraciiform or labriform modes have often rigid bodies, like our body and head modules. The caudal fin activated by the body module can be used as a rudder like in labriform mode. Hybrid propulsion (caudal and pectoral) can also be implemented like in ostraciiform mode. However, the concept of the robot is modular and additional modules could easily be added, e.g. to form a longer body made of a chain of a few modules. Indeed, we reused for this project modules that were initially used to construct amphibious snake and salamander robots (Crespi and Ijspeert 2006; Ijspeert et al. 2007).

Casings are molded in polyurethane lightened with glass microballs. Specific O-rings and grease are used to make the robot waterproof. Total robot's length is 25 cm. The density is slightly higher than that of water and a floater is added to adjust its density to just below 1000 kg/m^3.

The fins are actuated by 2.83 Watt Faulhaber DC motors and purpose-made gearboxes (reduction factors of 60 and 125 for the pectoral and caudal fins respectively). Pectoral fins can make complete rotations, while the motion of the caudal fin is limited to $\pm 60°$. The fins are made of 2-mm thick PE plates. The caudal fin has an aspect ratio of 2.9 for 35 cm^2, while pectoral fins have 0.6 for 50 cm^2. The fins can very easily be changed.

The robot is normally used without tether, except for long-term experiments (when batteries need to be recharged) as for the public exhibition presented in Sect. 6.

3.2 Electronics and sensors

Each fin is controlled by a PD motor controller, based on a PIC16F876A microcontroller which drives three SI9986 H-bridges. The motors have an integrated incremental encoder with 512 steps per turn, the signal of which is filtered and decoded by a LS7084 quadrature detector. The motor controllers are slaves on a I^{2}C bus, whose master is a PIC18F2580 microcontroller running at 40 MHz and placed in the head element. This microcontroller runs the locomotion controller (see next section).

Each motor module is powered by a 4.2 V Li-Ion battery, which is constantly recharged when external power is applied through a tether to the robot. As the master microcontroller is mounted on the PCB of a motor element inside the head, it also shares its battery. The motors are directly powered using the battery, whereas the electronics are supplied with 5 V, locally generated using a capacitive step-up converter.

Light, touch, and water sensors are placed in the front of the head in an interchangeable part. The two light sensors are placed in the horizontal plane, into transparent polymer tubes fixed at an angle of 60° from one another; a light filter is fixed around the tube and can be easily replaced depending on the environment. The water sensor is simply made of two electrical contacts that provide an *on* signal when the robot is immersed in water (due to water conduction) and an *off* signal otherwise. A two axis accelerometer (ADXL203) measures accelerations along the roll and pitch axes.

Note that our robot is relatively simple and that robots with more sophisticated pectoral fins have been developed, see for instance Kato (2005), Kato et al. (2005, 2006).

4 Locomotion control

The locomotion controller is composed of a CPG model for producing coordinated oscillations extended by a finite state machine for modulating the CPG activity and implementing various locomotor behaviors.

4.1 CPG model

Our locomotion controller is based on a CPG model implemented as a system of three coupled amplitude-controlled phase oscillators, one per fin (Fig. 4). We have used a similar CPG model in our lamprey/snake and salamander robots, although with different topologies of oscillator networks (Ijspeert and Crespi 2007; Ijspeert et al. 2007). An oscillator i is implemented as follows:

$$\dot{\phi}_i = \omega_i + \sum_j (w_{ij}\, r_j \sin(\phi_j - \phi_i - \varphi_{ij})), \tag{1}$$

$$\ddot{r}_i = a_r \left(\frac{a_r}{4}(R_i - r_i) - \dot{r}_i \right), \tag{2}$$

$$\ddot{x}_i = a_x \left(\frac{a_x}{4}(X_i - x_i) - \dot{x}_i \right), \tag{3}$$

$$\theta_i = x_i + r_i \cos(\phi_i) \tag{4}$$

where θ_i is the oscillating set-point (in radians) extracted from the oscillator, and ϕ_i, r_i, and x_i are state variables that encode respectively the phase, the amplitude, and the offset of the oscillations (in radians). The parameters ω_i, R_i, and X_i are control parameters for the desired frequency, amplitude and offset of the oscillations. The parameters w_{ij} and φ_{ij} are respectively coupling weights and phase biases which determine how oscillator j influences oscillator i. The parameters a_r and a_x are constant positive gains ($a_r = a_x = 20$ rad/s). The reference position (i.e., corresponding to a zero offset) for the pectoral fins is when these fins are turned backwards in a horizontal position. The reference position for the caudal fin is when that fin is in the sagittal plane.

These equations were designed such that the output of the oscillator θ_i exhibits limit cycle behavior, i.e., produces a stable periodic output. Equation 1 determines the time evolution of the phases of the oscillators. In this article, we use the same frequency parameter $\omega_i = \omega$ for all oscillators. The coupling parameters are $w_{ij} = 0.5$ [1/s], $\varphi_{ij} = 0.0$ [1/s] for all $i \neq j$ and $w_{ii} = 0.0$ [1/s], $\varphi_{ii} = 0.0$ [1/s] otherwise (i.e., there are no self-couplings). Oscillators 1,2,3 respectively correspond to the left-pectoral, right-pectoral, and caudal fins. With these parameters, the phases will converge to a regime in which the phases grow linearly with a common rate ω and with a zero phase difference between all three oscillators (i.e., $\Delta\phi_{ij} = \varphi_{ij} = 0.0$) from almost any initial conditions.[2]

Equations (2) and (3) are critically damped second order linear differential equations which have respectively R_i and X_i as stable fixed points. From any initial conditions, the state variables r_i and x_i will asymptotically and monotonically converge to R_i and X_i. This allows one to smoothly modulate the amplitude and offset of oscillations.

With these settings, the CPG therefore asymptotically converges to a limit cycle $\theta_i^{\infty}(t)$ for the i^{th} actuated joint that is defined by the following closed form solution:

$$\theta_i^{\infty}(t) = X_i + R_i \cdot \cos(\omega t + \phi_0) \tag{5}$$

where ϕ_0 depends on the initial conditions of the system. This means that the system stabilizes into oscillations that are synchronous for all three degrees of freedom, and that can be modulated by 7 control parameters, namely ω for setting the common frequency, R_i ($i \in \{1, 2, 3\}$) for setting the individual amplitudes, and X_i ($i \in \{1, 2, 3\}$) for setting the individual offsets. Figure 3 illustrates how the system converges to the stable oscillations starting from random initial conditions and after a random perturbation.

Such a CPG model has several nice properties. The first interesting property is that the system exhibits limit cycle behavior, i.e., oscillations rapidly return to the steady-state oscillations after any transient perturbation of the state variables (Fig. 3). The second interesting property is that this limit cycle has a closed form solution.[3] The function is sine-based and has control parameters (ω, R_i, and X_i) that are explicit and are directly related to relevant features of the oscillations. This facilitates the design of locomotion controllers. A third interesting property is that these control parameters can be abruptly and/or continuously varied while inducing only smooth modulations of the set-point oscillations (i.e., there are no discontinuities nor jerks). This property will extensively be used in the Results section for varying the locomotor behaviors (Sect. 5). Finally, a fourth interesting feature is that feedback terms can be added to (1–3) in order to maintain entrainment between control oscillations and mechanical movements (however this will not be explored in this article).

[2] The only exceptions are initial conditions in which two oscillators i, j are exactly in phase, i.e., $\Delta\phi_{ij} = \phi_j - \phi_i = 0$, and the third oscillator k is exactly in antiphase, i.e., $\Delta\phi_{ik} = \pi$. For those conditions, the system evolves to a regime which keeps these particular phase differences. In other words, this particular case represents an unstable fixed point for the differential equations that determine the time evolution of the phase differences.

[3] Very few types of oscillators have a closed form solution for their limit cycle.

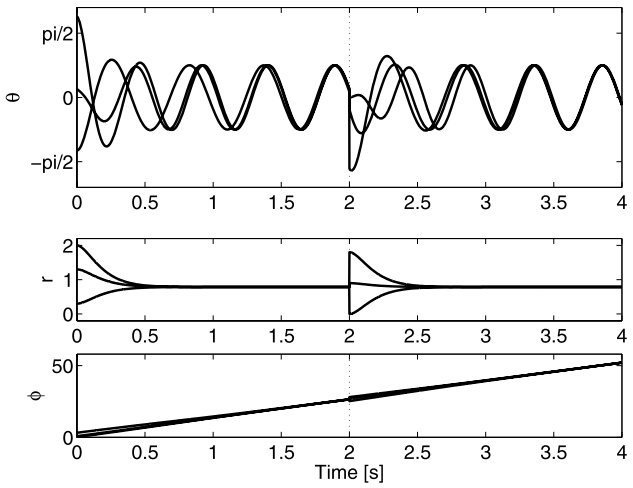

Fig. 3 Limit cycle behavior of the CPG. Starting from random initial conditions, the system quickly stabilizes in synchronous oscillations with controlled amplitude. At $t = 2$ s, random perturbations are applied to the state variables ϕ_i and r_i, and the system rapidly returns to the steady state oscillations

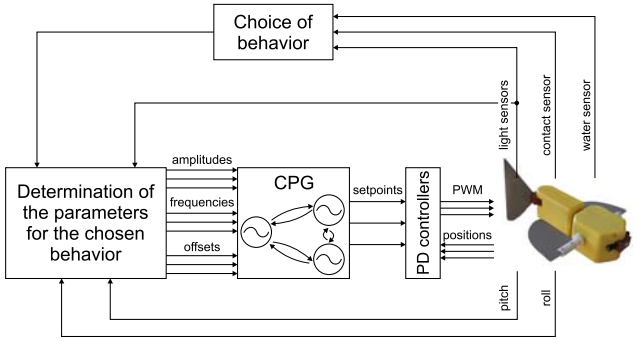

Fig. 4 Diagram of the complete control architecture. While using a predefined behavior the values from light sensors are not used. The values of pitch and roll were not used during the experiments described in this paper

4.2 Complete control architecture

The diagram of the complete control architecture is given in Fig. 4. The CPG model produces the set-points θ_i for PD controllers of the three fins. Different locomotor behaviors can be obtained by modulating the CPG control parameters ω, R_i, and X_i for the three fins.

Examples of locomotor behaviors include:

- Swimming *forwards*, by oscillating only the caudal fin, both pectoral fins, or all fins, with all offsets X_i set to zero.
- Swimming *backwards*, by turning the pectoral fins forward (i.e., by setting the pectoral offsets X_1 and X_2 to π) and stopping the oscillations of the caudal fin ($R_3 = 0$).
- *Spinning* around the roll axis, by setting the pectoral offsets X_1 and X_2 to $\pi/2$ and $-\pi/2$ (i.e., by turning one pectoral fin up and the other down).
- *Turning* (around the yaw axis) while swimming, by having a non zero offset X_3 for the caudal fin.
- *Turning on the spot*, by oscillating the pectoral fins, with one of the pectoral offset to π.
- Swimming *up* (or *down*), by setting an offset for both pectoral fins ($X_1 = X_2$) between 0 and $\pi/2$ ($-\pi/2$), proportionally to the desired vertical speed.
- *Crawling*, by stopping the oscillations of the fins ($R_1 = R_2 = R_3 = 0$), and applying a continuously increasing offset (X_1 and X_2) to both pectoral fins. Two possibilities are with $X_1 = X_2$ (both pectoral fins rotate in phase) or $X_1 = X_2 + \pi$ (pectoral fins rotate in anti-phase).

For all these behaviors, the speed of locomotion can be varied by adjusting the frequency ω and/or the amplitudes R_i of oscillations. Typically the speed of locomotion increases with those parameters until the torque limits of the motors are reached.

We made two types of experiments for testing these different locomotor behaviors. In a first set of experiments, the choice of behavior is done sequentially in a prefixed order without sensory inputs to test the different locomotor behaviors and the transitions between them.

In a second set of experiments, the behavior controller is programmed as a finite state machine to implement a simple phototaxis both in water and on the ground. A strong halogen lamp is used as a movable light source and a behavior is chosen on the basis of the values of both light sensors and of the water sensor. The default behavior is to track the light. But if the robot is not in water, it starts to crawl. If the light sensors' signal is too weak, it turns on the spot until it finds the light source again. And if the signals are saturated (i.e., the robot is too close to the lamp), the robot stops. When a contact with an obstacle is detected with the front touch sensor, the backwards behavior overrides all other behaviors for a few seconds.

Once a behavior has been chosen, a second finite state machine determines the 7 control parameters (common frequency, and amplitude and offset of each motor) to obtain that behavior. For example, if light tracking is chosen, the speed of the robot is controlled inversely proportionally to the amplitude of light by adjusting both the frequency (6) and the amplitude of the oscillations (7). The caudal offset is controlled proportionally to the difference of light (8).

$$\omega_i = k_{\omega i} \frac{1}{l_1 + l_2} \quad i = 1, 2, 3, \tag{6}$$

$$R_i = k_{Ri} \frac{1}{l_1 + l_2} \quad i = 1, 2, 3, \tag{7}$$

$$X_3 = k_{X3}(l_1 - l_2) \quad X_1 = 0, X_2 = 0 \tag{8}$$

where the k_{ij} are gains of the regulator and l_1, l_2 the amplitudes of the two light sensors. Note that the CPG never

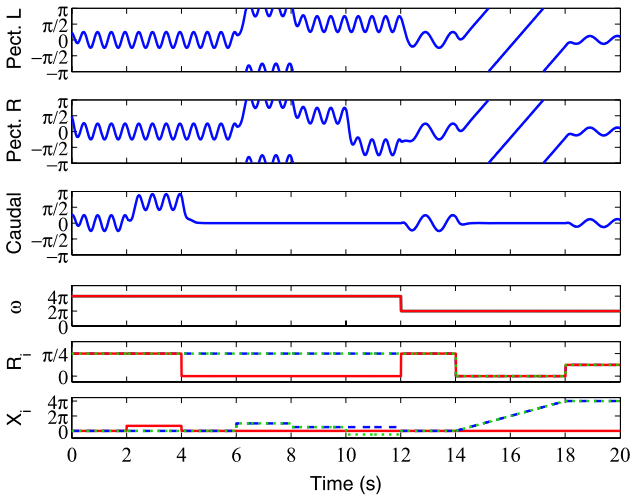

Fig. 5 Sequence of different locomotor behaviors. The graphs show the set-points in radians sent to the three fins. See text for details

needs any resetting and is continuously running while the control parameters are modified.

5 Results

5.1 Sequentially testing the locomotor behaviors

We tested the ability of the CPG to produce the different types of locomotor behaviors presented above. Figure 5 presents a sequence of transitions from one behavior to the other. In that sequence, the CPG makes transitions between swimming straight with both pectoral and caudal fins ($t \leq 2$ s), turning with a caudal offset ($2 < t \leq 4$ s), swimming straight with only pectoral fins ($4 < t \leq 6$ s), swimming backwards ($6 < t \leq 8$ s), swimming upwards ($8 < t \leq 10$ s), rolling ($10 < t \leq 12$ s), slow swimming straight with pectoral and caudal fins ($12 < t \leq 14$ s), crawling ($14 < t \leq 18$ s), and swimming straight with small amplitudes ($18 < t \leq 20$ s). Figure 6 illustrates forward swimming with pectoral fins. Figure 7 shows the straight forward crawling gait obtained using $X_1 = X_2$. If only one pectoral fin is actuated the robot crawls to the left or right. With $X_1 = X_2 + \pi$, it crawls forward zigzagging.

Figure 8 shows a turning maneuver by modulating the offset of the tail fin (turn to the right followed by a turn to the left). The minimal radius of turning for this type of turning (with caudal offset) is 0.12 m. Even sharper turns can be made with the *turning on the spot* maneuver. Movies of the robot can be viewed at http://birg2.epfl.ch/boxybot.

All these transitions are obtained with abrupt changes of the control parameters ω, R_i, and X_i. Despite these abrupt changes, smooth oscillations are produced by the CPG (as shown on Fig. 5). Note also that all oscillations remain phase-locked with a zero phase difference thanks to the inter-oscillator couplings.

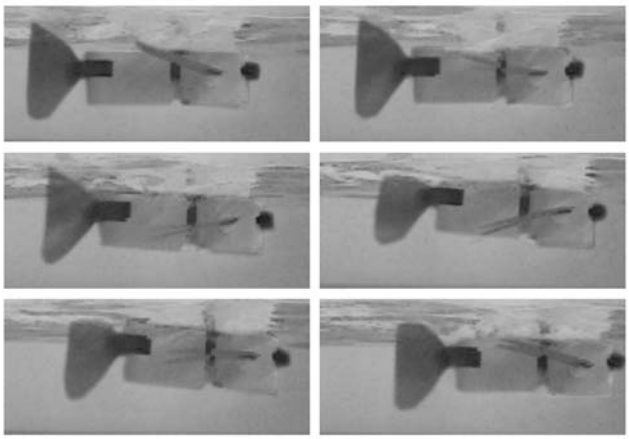

Fig. 6 Snapshots of swimming forwards with both pectoral fins (from *top left* to *bottom right*)

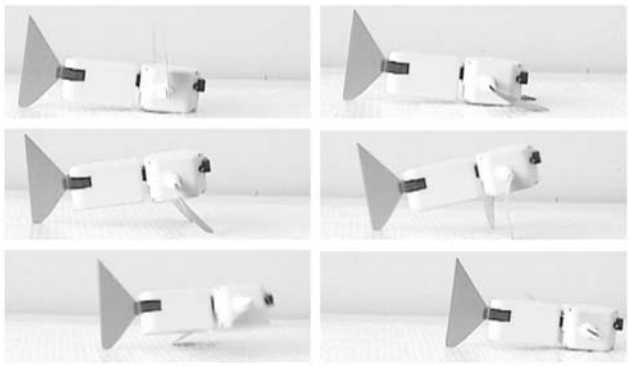

Fig. 7 Snapshots of crawling using continuous rotation of pectoral fins $X_1 = X_2$ (from *top left* to *bottom right*)

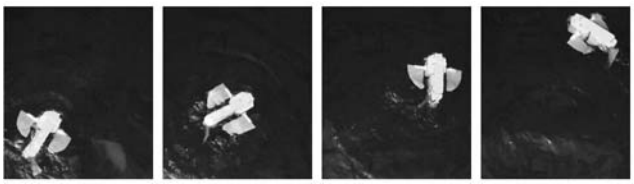

Fig. 8 Snapshots of turning transition

5.2 Evaluating the speed of locomotion

The speed of locomotion can be adjusted by gradually increasing both the frequency and/or amplitude parameters of the CPG. Figure 9 shows the activity of the CPG when both are increased simultaneously.

In order to test how the speed of locomotion depends on the frequency and amplitude of oscillations, we carried out a series of swimming tests. Steady-state speed was measured at different levels of frequencies and amplitudes of all fins.

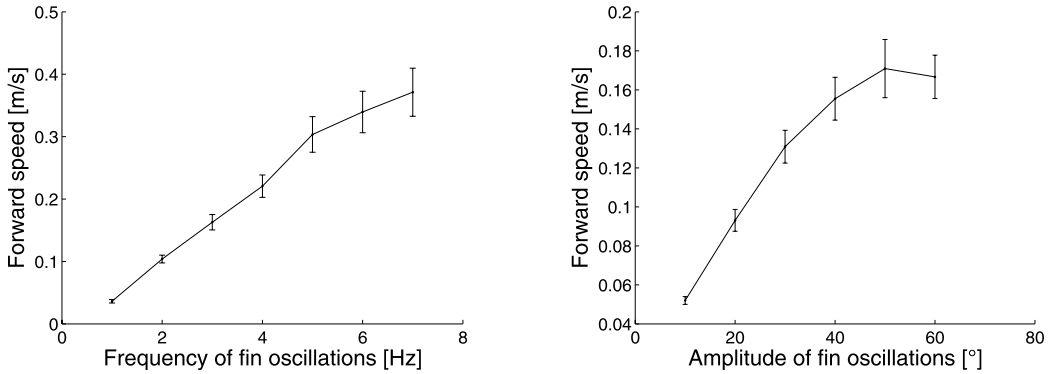

Fig. 10 Variation of forward speed with pectoral fins. On the *left*, variation with oscillations frequency at a fixed amplitude of 20°. On the *right*, variation with oscillation amplitude at a fixed frequency of 2 Hz. Speed is obtained from the measure of distance covered and time using video recordings. Error bars are calculated from the estimated precision of those two measures (±0.02 m for the distance and ±0.08 s for the time)

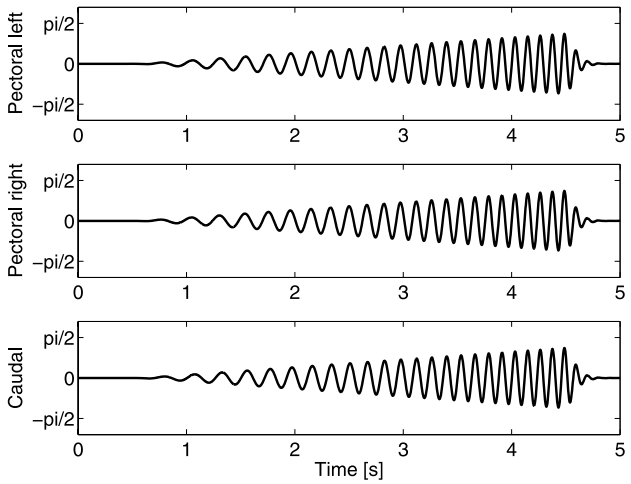

Fig. 9 Acceleration during swimming

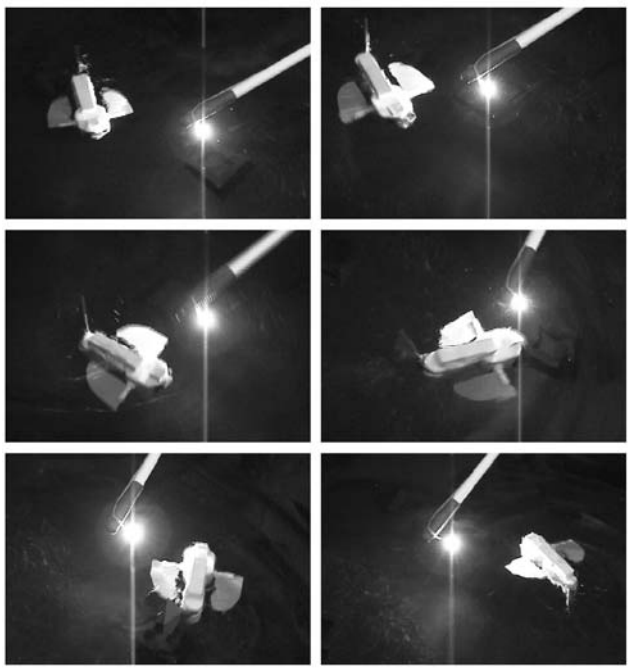

Fig. 11 Snapshots of phototaxis during swimming (from *top left* to *bottom right*)

Figure 10 shows the results for variations of frequency at a fixed amplitude (on the left) and for variations of amplitude at a fixed frequency (on the right). As could be expected, the speed of swimming increases with the frequency until the motors reach their torque limits. Similarly, at a fixed frequency, the speed of swimming increases with the amplitude until the oscillations become too large (larger than 50°) and create braking waves. Overall, the robot can swim up to 0.37 m/s (i.e., 1.4 body lengths per second) at a frequency of 8 Hz and amplitudes of ±40° with both pectorals and caudal fins.

5.3 Phototaxis

Using the phototaxis behavior described in Sect. 4.2, the fish robot is able to reach a static bright light (brighter than the environment) from a maximal distance of 50 cm and to keep station near the light. It is also able to follow a light that moves slowly (Fig. 11). If the light moves too quickly on the side, the robot cannot track it because the control law for choosing the speed and caudal offset is very basic (only proportional gains are used). The robot is programmed to then slowly turn on itself until the light comes into view again, in which case it resumes the light tracking behavior. The same phototaxis behavior is also implemented on ground (Fig. 12).

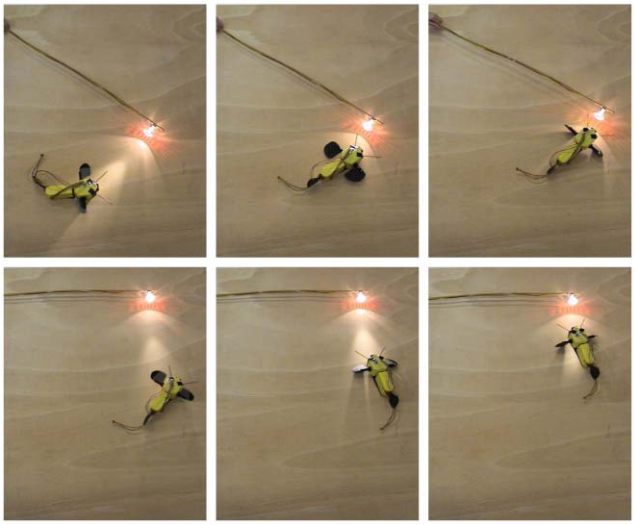

Fig. 12 Snapshots of phototaxis during crawling (from *top left* to *bottom right*)

Fig. 13 BoxyBot in its aquarium at the exhibition (picture: Alain Herzog)

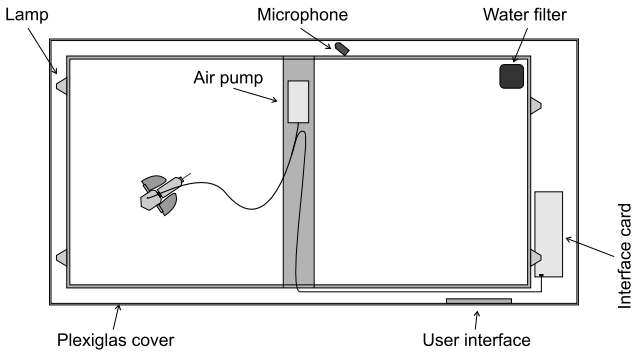

Fig. 14 Schematic drawing of the whole setup (top view)

6 Public exhibition

Since March 2006 BoxyBot is part of a public exhibition ("forum découvertes") at the School of Computer and Communication Science at EPFL (Fig. 13). The aim of this exhibition is to present some research projects carried out in the school to the general public. The robot stays day and night in an aquarium and different means of interacting with it are provided to the visitors. The robot is programmed with essentially the same control architecture as used in the previous experiments (Fig. 4) with the exception that the robot is permanently connected through a tether to an offboard PC for monitoring and for receiving information from external sensors (see next sections). The batteries are also permanently recharged through that tether to allow the robot to be active 16 hours per day. Because of this the robot is not truly autonomous anymore. For us the purpose of this exhibition is to demonstrate that the CPG-based control architecture is well suited for interactive control with a human in the loop. The exhibition is also a demonstration that the robot is robust enough for long and extensive use.

The environment is an aquarium (150×75 cm) filled with approx. 30 cm of water, inside which the fish robot swims. Four halogen lamps are placed externally to the aquarium, near the corners of the short side. The whole setup is protected by a plexiglas cover, which restricts the visitors from directly manipulating it.

6.1 Hardware description

The overall structure of the system is depicted in Figure 14. A standard aquarium filter is placed inside the aquarium to constantly clean the water; moreover, a small amount of sodium hypochlorite is added to avoid the development of algae. A fan is placed on the top of the plexiglas cover to remove the moisture, thus avoiding the formation of condensation.

The robot is connected to an interface card through a 5-wire cable and a rotating contact. The cable supplies the robot with external power when needed (24 V), has a signal to completely turn off the robot (i.e., to disconnect the batteries from the circuits) and also contains the I^2C signals used for communication. The external voltage level of 24 V has been chosen to minimize the current on the connection wires, which have a limited section. A small aquarium pump injects low pressure air inside the robot (through a highly flexible silicone tube) to avoid water leakages.[4]

The interface card is based on a PIC18F6622 microcontroller, configured as an I^2C slave and connected to the internal bus of the robot through an I^2C driver (the internal drivers of the PIC are too weak, due to the cable length).

[4]The robot is normally waterproof, but for long term usage (e.g. over several months) the increased air pressure inside the robot helps preventing leakages which were inevitably occurring without it. The internal pressure also helps identifying possible leakage points, since these become visible through air bubbles.

The software on the microcontroller implements a register bank that can be read and written both over I^2C and using a RS-232 line connected to a PC. The interface card is powered with a 24 V switching power supply, whose output is also supplied to the robot through a relay. The card has four other relays (used to power the halogen lights), which are connected to a 12 V transformer. The state of all the relays is directly controlled by one of the registers implemented on the microcontroller, and can thus be read and modified both by the robot and by the control PC.

Three buttons, implemented as capacitive touch sensors connected to the interface card, are fixed inside the plexiglas cover to implement a simple user interface (see next section).

A small microphone connected to the PC is placed at the side of the aquarium to detect when users knock on the cover. The detection is done with a very simple but effective threshold function on the average intensity of the sound.

6.2 User interaction

Visitors can interact with the robot in several ways: (1) by turning on the lights located around the aquarium, (2) by forcing the robot to perform a particular action by pressing a button, and (3) by knocking on the plexiglas cover. One of the buttons cyclically turns on one of the lights. By pressing it, the user can therefore induce the phototaxis behavior. When one of the lights is turned on, the robot swims in its direction using the light sensors, and turns it off (using the communication with the interface card) when touching the border of the aquarium in front of the light. The two other buttons allow the user to force the robot to perform two particular behaviors: diving to the bottom of the aquarium and swimming backwards. Knocks on the plexiglas cover are detected and are also used for interacting with the system: a single hit triggers a temporary acceleration of the swimming speed, and a double hit triggers the spinning behavior. When no user input is detected, the robot is programmed to randomly switch between the different locomotor behaviors described in Sect. 4.2. When no user activity is observed for more than two minutes, the robot is automatically turned off, and is reactivated when any type of activity is detected.

The amount of time the robot is active each day is counted by the monitoring PC and plotted in Fig. 15. During peak days, the robot has been active up to almost 6 hours per day.

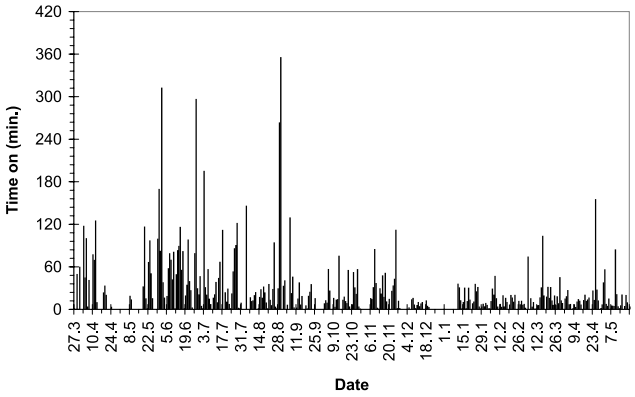

Fig. 15 Daily robot activity plot

7 Discussion

BoxyBot has demonstrated its capacity of maneuverability. Using only three fins, it can move in 3D with different types of maneuvers and go out of water using a crawling gait. It can avoid obstacles by going backwards for a few seconds. Finally, the robot can reach a bright light and follow it slowly.

The main purpose of this article was to demonstrate that the CPG model can be very useful for the online generation of the fin trajectories. The CPG provides the possibility to abruptly change control parameters while ensuring smooth variations of behavior. Producing continuous and smoothly varying set-points is indeed important to limit mechanical damage to the motors and gearboxes, but also to avoid jerks that could destabilize the swimming and crawling gaits. But note that producing too smooth trajectories might be counterproductive when rapid accelerations or changes of attitude are needed. The reaction time is determined by the gains a_r and a_x (the higher these gains, the faster the response), and these gains should be properly adjusted to a particular robot and task (possibly during runtime). In addition to smooth response, the phototaxis experiment showed that the CPG model can be continuously modulated and can therefore readily be used by higher level behavior controllers. This is not unlike locomotion control in vertebrate animals where CPGs in the spinal cord produce the rhythmic patterns necessary for locomotion, and higher control centers such as the motor cortex and the cerebellum generate signals for the modulation of speed and direction.

The presentation of BoxyBot at the *forum découvertes* exhibition showed that the robot is able to swim for long periods of time (currently, 616 days). The waterproofing problems which were present during the first weeks were solved with the addition of the external air pump, as correcting them mechanically would imply modifications on the molded parts. Moreover, the possibility for any unexperienced user to control the robot behavior demonstrates the validity of the CPG approach for interactive robot locomotion with a human in the loop. However, a detailed comparative study with other methods, for instance the control laws developed by Kato's group (Kato 2005; Kato et al. 2005, 2006), needs to be done in order to assess whether the CPG

method really offers an interesting alternative to these methods.

We will extend this work in several directions. First of all, we will explore whether our CPG can be designed to use simpler command signals for initiating and modulating locomotion. In vertebrates, simple tonic (i.e., non-oscillating) signals are sufficient to modulate the speed of locomotion and even to induce gait transitions. In our model, several control parameters need to be changed simultaneously to obtain certain transitions of behavior, and we would like to see if this could be simplified. Another point that we intend to explore is whether more complex signal shapes could lead to more efficient swimming. We currently use harmonic (i.e., sine-like) oscillations, and it might be that relaxation-like oscillations (i.e., oscillations that have both a fast and a slow mode) provide faster locomotion for similar frequencies and amplitudes. This will require the use of other types of oscillators in the CPG model (or of filters for modifying the amplitude control oscillators' outputs). Finally, we would like to explore the integration of sensory feedback in the CPG (not only through modulation of the control parameters as done during the phototaxis experiment and for the public exhibition). In the lamprey, for instance, stretch receptors in the spinal cord ensure that the travelling neural wave remains coordinated with the travelling mechanical wave, and rhythms in the CPG synchronize with externally forced movements of the tail. The CPG model can easily be extended to include similar types of sensory feedback, and we will explore the benefits of such entrainment phenomenon.

Acknowledgements We gratefully acknowledge the technical support of André Guignard and André Badertscher for the design and the construction of the robot. We also would like to acknowledge Sacha Constantinescu for his contribution in designing the light sensors, and Fabien Vannel for the design of the touch sensors used for the exhibition. This work was made possible thanks to the financial support from the Swiss National Science Foundation.

References

Arena, P. (2001). A mechatronic lamprey controlled by analog circuits. In *Proceedings of the 9th IEEE mediterannean conference on control and automation (MED '01)*.

Billard, A., & Ijspeert, A. J. (2000). Biologically inspired neural controllers for motor control in a quadruped robot. In *Proceedings of the IEEE-INNS-ENNS international joint conference on neural networks—IJCNN2000* (Vol. VI, pp. 637–641).

Colgate, J. E., & Lynch, K. M. (2004). Mechanics and control of swimming: A review. *IEEE Journal of Oceanic Engineering*, *29*(3), 660–673.

Crespi, A., & Ijspeert, A. J. (2006). AmphiBot II: An amphibious snake robot that crawls and swims using a central pattern generator. In *Proceedings of the 9th international conference on climbing and walking robots (CLAWAR 2006)*.

Delcomyn, F. (1980). Neural basis for rhythmic behaviour in animals. *Science*, *210*, 492–498.

Deng, X., & Avadhanula, S. (2005). Biomimetic micro underwater vehicle with oscillating fin propulsion: System design and force measurement. In *Proceedings of the 2005 IEEE international conference on robotics and automation (ICRA 2005)* (pp. 3312–3317).

Fukuoka, Y., Kimura, H., & Cohen, A. H. (2003). Adaptive dynamic walking of a quadruped robot on irregular terrain based on biological concepts. *The International Journal of Robotics Research*, *22*(3–4), 187–202.

Grillner, S. (1985). Neural control of vertebrate locomotion – central mechanisms and reflex interaction with special reference to the cat. In W. J. P. Barnes & M. H. Gladden (eds.), *Feedback and motor control in invertebrates and vertebrates* (pp. 35–56). Croom Helm.

Ijspeert, A. J., & Crespi, A. (2007). Online trajectory generation in an amphibious snake robot using a lamprey-like central pattern generator model. In *Proceedings of the 2007 IEEE international conference on robotics and automation (ICRA 2007)* (pp. 262–268).

Ijspeert, A. J., Crespi, A., & Cabelguen, J. M. (2005). Simulation and robotics studies of salamander locomotion. Applying neurobiological principles to the control of locomotion in robots. *Neuroinformatics*, *3*(3), 171–196.

Ijspeert, A. J., Crespi, A., Ryczko, D., & Cabelguen, J.-M. (2007). From swimming to walking with a salamander robot driven by a spinal cord model. *Science*, *315*(5817), 1416–1420.

Kato, N. (2000). Control performance in the horizontal plane of a fish robot with mechanical pectoral fins. *IEEE Journal of Oceanic Engineering*, *25*(1), 121–129.

Kato, N. (2005). Median and paired fin controllers for biomimetic marine vehicles. *Applied Mechanics Reviews*, *58*(4), 238–252.

Kato, N., Liu, H., & Morikawa, H. (2005). Biology-inspired precision maneuvering of underwater vehicles—part 3. *International Journal of Offshore and Polar Engineering*, *15*(2), 81–87.

Kato, N., Ando, Y., Shigetomi, T., & Katayama, T. (2006). Biology-inspired precision maneuvering of underwater vehicles (part 4). *International Journal of Offshore and Polar Engineering*, *16*(3), 195–201.

Lachat, D., Crespi, A., & Ijspeert, A. J. (2006). Boxybot: A swimming and crawling fish robot controlled by a central pattern generator. In *Proceedings of the first IEEE/RAS-EMBS international conference on biomedical robotics and biomechatronics (BioRob 2006)*.

Liu, J., Dukes, I., Knight, R., & Hu, H. (2004). Development of fish-like swimming behaviours for an autonomous robotic fish. In *Proceedings of control 2004*.

Liu, J., Dukes, I., & Hu, H. (2005). Novel mechatronics design for a robotic fish. In *Proceedings of the 2005 IEEE/RSJ international conference on intelligent robots and systems (IROS 2005)* (pp. 807–812).

Nakanishi, J., Morimoto, J., Endo, G., Cheng, G., Schaal, S., & Kawato, M. (2004). An empirical exploration of phase resetting for robust biped locomotion with dynamical movement primitives. In *Proceedings of the 2004 IEEE/RSJ international conference on intelligent robots and systems (IROS 2004)* (pp. 919–924).

Righetti, L., & Ijspeert, A. J. (2006). Programmable central pattern generators: an application to biped locomotion control. In *Proceedings of the 2006 IEEE international conference on robotics and automation (ICRA 2006)*.

Sfakiotakis, M., Lane, D. M., & Davies, J. B. C. (1999). Review of fish swimming modes for aquatic locomotion. *IEEE Journal of Oceanic Engineering*, *24*(2), 237–252.

Stefanini, C., Orlandi, G., Menciassi, A., Ravier, Y., La Spina, G., Grillner, S., & Dario, P. (2006). A mechanism for biomimetic actuation in lamprey-like robots. In *Proceedings of the first IEEE/RAS-EMBS international conference on biomedical robotics and biomechatronics (BioRob 2006)* (pp. 579–584).

Triantafyllou, M. S., & Triantafyllou, G. S. (1995). An efficient swimming machine. *Scientific American*, *272*(3), 40–48.

Wilbur, C., Vorus, W., Cao, Y., & Currie, S. N. (2002). In *Neurotechnology for biomimetic robots*. *A Lamprey-based undulatory vehicle*. Cambridge/London: Bradford/MIT Press.

Yu, J., Tan, M., Wang, S., & Chen, E. (2004). Development of a biomimetic robotic fish and its control algorithm. *IEEE Transactions on Systems, Man, and Cybernetics, Part B: Cybernetics*, *34*(4), 1798–1810.

Alessandro Crespi is a postdoctoral researcher at the Biologically Inspired Robotics Group (BIRG) at EPFL. He has a B.Sc./M.Sc. and Ph.D. in computer science from the EPFL. His research interests are in the field of biologically inspired amphibious robots. He is mainly working on the development of the electronics of the robots, and on the experiments to characterize their locomotion.

Daisy Lachat obtained her M.Sc. in Microengineering in 2006 from the EPFL. She now works as development engineer in the industry.

Ariane Pasquier obtained her M.Sc. in Computer Science in October 2007 from the EPFL. She now works as a Development Engineer at Swissquote Bank.

Auke Jan Ijspeert is an assistant professor at the EPFL (the Swiss Federal Institute of Technology at Lausanne), and head of the Biologically Inspired Robotics Group (BIRG). He has a B.Sc./M.Sc. in physics from the EPFL, and a Ph.D. in artificial intelligence from the University of Edinburgh. His research interests are at the intersection between robotics, computational neuroscience, nonlinear dynamical systems, and applied machine learning. He is interested in using numerical simulations and robots to get a better understanding of sensorimotor coordination in animals, and in using inspiration from biology to design novel types of robots and adaptive controllers. With his colleagues, he has received the Best Paper Award at ICRA2002, the Industrial Robot Highly Commended Award at CLAWAR2005, and the Best Paper Award at the IEEE-RAS Humanoids 2007 conference. He was the Technical Program Chair of 5 international conferences (BioADIT2004, SAB2004, AMAM2005, BioADIT2006, LATSIS2006), and has been a program committee member of over 30 conferences.